

JOINT LIFETIME MODELLING WITH MATRIX DISTRIBUTIONS

HANSJÖRG ALBRECHER, MARTIN BLADT, AND ALARIC J.A. MÜLLER

ABSTRACT. Acyclic phase-type (PH) distributions have been a popular tool in survival analysis, thanks to their natural interpretation in terms of ageing towards its inevitable absorption. In this paper, we consider an extension to the bivariate setting for the modelling of joint lifetimes. In contrast to previous models in the literature that were based on a separate estimation of the marginal behavior and the dependence structure through a copula, we propose a new time-inhomogeneous version of a multivariate PH class (mIPH) that leads to a model for joint lifetimes without that separation. We study properties of mIPH class members and provide an adapted estimation procedure that allows for right-censoring and covariate information. We show that initial distribution vectors in our construction can be tailored to reflect the dependence of the random variables, and use multinomial regression to determine the influence of covariates on starting probabilities. Moreover, we highlight the flexibility and parsimony, in terms of needed phases, introduced by the time-inhomogeneity. Numerical illustrations are given for the famous data set of joint lifetimes of Frees et al. [12], where 10 phases turn out to be sufficient for a reasonable fitting performance. As a by-product, the proposed approach enables a natural causal interpretation of the association in the ageing mechanism of joint lifetimes that goes beyond a statistical fit.

1. INTRODUCTION

When studying insurance products on multiple lives, it is natural to assume that individuals who are exposed to very similar life conditions may have somewhat correlated lifetimes. This is especially true for married couples, since, once married, the spouses typically share to a large extent a similar lifestyle. Indeed, the simplistic assumption of independence of lifetimes of partners has been shown to be inappropriate in various papers. For example, Frees et al. [12] used different bivariate (copula) models to assess the effect of dependency between husband and wife on insurance annuities, illustrating their approach on a by now classical data set of a large insurer. For that same data set, Luciano et al. [16] captured the dependence between survival times of spouses by an Archimedean copula, whose marginals were estimated according to a stochastic intensity approach. In a similar spirit, Dufresne et al. [11] let the Archimedean copula parameter depend on the age difference of partners at issue of the policy, in order to describe the dependence of the remaining lifetime of a couple. In Gobbi et al. [13], extended Marshall-Olkin models were employed for that same data set, where the continuous copula approach is extended by allowing for fatal events that affect both marginal lives.

In this paper we propose an alternative to copula-based methods for the modelling of joint remaining lifetimes in a couple based on multivariate phase-type distributions. Phase-type (PH) distributions are interesting candidates since they broaden favourable properties of

Key words and phrases. Mortality Modelling, multivariate PH distributions, censoring, EM algorithm.

exponential random variables to scenarios where the latter alone would not be appropriate. In particular, the denseness of PH distributions among all distributions on the positive half-line in the sense of weak convergence, which extends to the multivariate setup, is a major advantage when one wants to approximate a distribution. For more details on PH distributions we refer readers to Bladt & Nielsen [7]. Opposed to copula-based methods, a PH distribution can give rise to a natural interpretation when used to approximate lifetime distributions. One can view the path of a Markov jump process as the life of an individual, which goes through several different states (for instance biological markers) before reaching the inevitable absorption (death) state. Along this interpretation, acyclic PH distributions have been the first choice for modelling the aging process of a human life, since they only allow forward transitions or direct exits to the absorption state. This characteristic makes them an appropriate tool for describing lifetimes ended by natural aging or accidents. In Lin & Liu [15], a PH distribution with Coxian structure was used to explain the physical aging process of marginal lifetimes. This approach was extended in Asmussen et al. [4] to generalised Coxian distributions for the purpose of pricing equity-linked products. The first contribution to lift the PH approach to bivariate lifetime models was Ji et al. [14], where a Markovian multi-state model and a semi-Markov model are used to describe the dependence between the lifetimes of husbands and wives. Spreeuw & Owadally [19] also use a Markovian multi-state model, with more attention given on how to tie the bereavement effect to forces of mortality. Moutanabbir & Abdelrahman [17] then used a bivariate Sarmanov distribution with PH marginals to model joint lifetimes. Both papers focused on the pricing of multiple-life insurance contracts.

Recently, Albrecher et al. [2] introduced time-inhomogeneous PH (IPH) distributions for the purpose of lifetime modelling, which leads to a considerable reduction of necessary phases for a satisfactory fit of given data, since the introduced inhomogeneity can more efficiently accommodate non-exponential shapes than an augmentation of the phase dimension. In particular, [2] applied regression on the intensity functions of the IPH distributions to associate lifetimes of different cohorts and populations.

In this paper, we propose a different route for using available information in the data set, namely to incorporate multinomial logistic regressions in the estimation procedure of multivariate PH distributions. In particular, the regression is applied to the initial distribution vectors of each IPH component, which adapts an approach presented in Bladt & Yslas [8] to the multivariate case. The resulting dependence structure allows for explicit formulas alongside an intuitive ‘ageing’ interpretation and, beyond the theoretical contribution, for a satisfactory fit to the bivariate spouses’ lifetime data.

The remainder of the paper is structured as follows. Section 2 introduces the class of multivariate PH distributions that we will use to describe joint lifetimes of couples; we also provide some additional properties. In Section 3 an estimation method for this multivariate PH distribution is introduced, which allows for right censoring and covariate information. Section 4 then applies and illustrates the procedure on the classical spouses’ lifetime data set from [12] and interprets the results. Section 5 concludes.

2. MULTIVARIATE PHASE-TYPE DISTRIBUTIONS

We first recall the mPH class, which was introduced in Bladt [6].

2.1. mPH distributions. Let $\{J_t^{(i)}\}_{t \geq 0}$, $i = 1, \dots, d$, denote separate homogeneous Markov pure-jump processes on the common state space $E = \{1, \dots, p, p+1\}$, with states $1, \dots, p$ being transient and $p+1$ absorbing. Defining transition probabilities as

$$p_{jl}^{(i)}(s, t) = \mathbb{P}(J_t^{(i)} = l | J_s^{(i)} = j), \quad 0 \leq j, l \leq p+1, \quad 0 < i \leq d,$$

we may write

$$\mathbf{P}_i(s, t) = \exp(\mathbf{\Lambda}_i(t-s)) = \begin{pmatrix} \exp(\mathbf{T}_i(t-s)) & \mathbf{e} - \exp(\mathbf{T}_i(t-s))\mathbf{e} \\ \mathbf{0} & 1 \end{pmatrix} \in \mathbb{R}^{(p+1) \times (p+1)},$$

for $s < t$, $0 \leq i \leq d$, where $\mathbf{\Lambda}_i(t)$ are intensity matrices. In the following we write \mathbf{e}_k for the k -th canonical basis vector in \mathbb{R}^p , $\mathbf{e} = \sum_{j=1}^p \mathbf{e}_j$, and

$$\mathbf{T}_i = \{t_{ks}^{(i)}\}_{k,s \in E}, \quad \mathbf{t}_i = -\mathbf{T}_i \mathbf{e} = (t_1^{(i)}, \dots, t_p^{(i)})^\top, \quad k = 1, \dots, p.$$

The crucial property of this class of PH distributions is now its dependence structure. Concretely, the assumption is that all jump processes start in the same state at time $t = 0$, but proceed independently thereafter until absorption. That is, dependence is introduced solely through the shared initial state, which leads to a particularly tractable yet flexible model class. More formally,

$$(2.1) \quad J_0^{(i)} = J_0^{(l)}, \quad \{J_t^{(i)}\}_{t \geq 0} \perp\!\!\!\perp_{J_0^{(1)}} \{J_t^{(l)}\}_{t \geq 0, l \neq i}, \quad \forall i, l \in \{1, \dots, d\}.$$

We will use $J_0 := J_0^{(i)}$ to simplify notation. Let $\mathbb{P}(J_0 = j) = \pi_j$, $j = 1, \dots, p$ and $\boldsymbol{\pi} = (\pi_1, \dots, \pi_p)$ denote the distribution vector of the shared initial state. The random variables

$$(2.2) \quad X_i = \inf\{t > 0 : J_t^{(i)} = p+1\}, \quad i = 1, \dots, d,$$

are then all univariate PH distributed. We say that the random vector $X = (X_1, \dots, X_d) \in \mathbb{R}_+^d$ has a multivariate phase-type distribution (mPH) if each marginal variable X_i , $i = 1, 2, \dots, d$ is given by (2.2) and pairwise dependence is defined by (2.1). We use the notation

$$X \sim \text{mPH}(\boldsymbol{\pi}, \mathcal{T}), \quad \text{with} \quad \mathcal{T} = \{\mathbf{T}_1, \dots, \mathbf{T}_d\}.$$

The joint cumulative distribution function of X is given by

$$\begin{aligned} F_X(x) &= \mathbb{P}(X_1 \leq x_1, X_2 \leq x_2, \dots, X_d \leq x_d) \\ &= \sum_{j=1}^p \mathbb{P}(X_1 \leq x_1, X_2 \leq x_2, \dots, X_d \leq x_d | J_0 = j) \mathbb{P}(J_0 = j) \\ &= \sum_{j=1}^p \pi_j \prod_{i=1}^d (1 - \mathbf{e}_j^\top \exp(\mathbf{T}_i x_i) \mathbf{e}), \quad x \in \mathbb{R}_+^d. \end{aligned}$$

Furthermore, the survival function is

$$S_X(x) = \mathbb{P}(X_1 > x_1, X_2 > x_2, \dots, X_d > x_d)$$

$$= \sum_{j=1}^p \pi_j \prod_{i=1}^d \mathbf{e}_j^\top \exp(\mathbf{T}_i x_i) \mathbf{e},$$

and the probability density function is given by

$$f_X(x) = \sum_{j=1}^p \pi_j \prod_{i=1}^d \mathbf{e}_j^\top \exp(\mathbf{T}_i x_i) \mathbf{t}_i.$$

For more details, cf. [6].

2.2. mIPH distributions. The particular focus in this paper will now be on an inhomogeneous extension of the mPH distribution (briefly mentioned in [6, Sec.6.1]). When considering time-inhomogeneous Markov pure jump processes on the common state-space E , it follows from Albrecher & Bladt [1] that the transition matrices are modified to

$$\mathbf{P}(s, t) = \prod_s^t (\mathbf{I} + \boldsymbol{\Lambda}(u) du) := \mathbf{I} + \sum_{k=1}^{\infty} \int_s^t \int_s^{u_k} \cdots \int_s^{u_2} \boldsymbol{\Lambda}(u_1) \cdots \boldsymbol{\Lambda}(u_k) du_1 \cdots du_k,$$

with sub-intensity matrix

$$\boldsymbol{\Lambda}(t) = \begin{pmatrix} \mathbf{T}(t) & \mathbf{t}(t) \\ \mathbf{0} & 0 \end{pmatrix} \in \mathbb{R}^{(p+1) \times (p+1)}, \quad t \geq 0.$$

The random variables $X_i = \inf\{t > 0 : J_t^{(i)} = p+1\}$, $i = 1, \dots, d$, then follow univariate inhomogeneous phase-type (IPH) distributions, cf. [1] for more details.

Here we focus on the particularly tractable case $\mathbf{T}_i(t) = \lambda_i(t) \mathbf{T}$. A random vector $X = (X_1, \dots, X_d)$ is said to have an inhomogeneous multivariate PH (mIPH) distribution if all marginals follow IPH distributions and the dependence structure is defined by (2.1). We write

$$X \sim \text{mIPH}(\boldsymbol{\pi}, \mathcal{T}, \mathcal{L}), \quad \text{where } \mathcal{T} = \{\mathbf{T}_1, \dots, \mathbf{T}_d\}, \quad \mathcal{L} = \{\lambda_1, \dots, \lambda_d\}.$$

With

$$g_i^{-1}(x) := \int_0^x \lambda_i(u) du, \quad i = 1, \dots, d,$$

the cumulative distribution function, survival function and density of X are given by

$$F_X(x) = \sum_{j=1}^p \pi_j \prod_{i=1}^d (1 - \mathbf{e}_j^\top \exp(\mathbf{T}_i g_i^{-1}(x_i)) \mathbf{e}), \quad x \in \mathbb{R}_+^d,$$

$$S_X(x) = \sum_{j=1}^p \pi_j \prod_{i=1}^d \mathbf{e}_j^\top \exp(\mathbf{T}_i g_i^{-1}(x_i)) \mathbf{e}, \quad x \in \mathbb{R}_+^d,$$

and

$$f_X(x) = \sum_{j=1}^p \pi_j \prod_{i=1}^d \mathbf{e}_j^\top \exp(\mathbf{T}_i g_i^{-1}(x_i)) \mathbf{t}_i \lambda_i(x_i), \quad x \in \mathbb{R}_+^d,$$

respectively. Note that one can view each IPH random variable as a transformation of a PH random variable (and correspondingly the absorption time of a time-transformed formerly

time-homogenous Markov jump process), with $Y \sim \text{PH}(\boldsymbol{\pi}, \mathbf{T})$ and $g(Y) \sim \text{IPH}(\boldsymbol{\pi}, \mathbf{T}, \lambda)$. The construction of $\text{mIPH}(\boldsymbol{\pi}, \mathcal{T}, \mathcal{L})$ allows different sub-intensity matrices and inhomogeneity functions for each marginal, as long as they share the same state-space. This leads to a considerable model flexibility. In particular, when compared to the homogeneous case, time-inhomogeneity allows for substantially smaller state-spaces for appropriate fits of data with potentially non-exponential tails (cf. [1]), and the mIPH class inherits this feature.

When we condition a mIPH distribution on one or more marginals, we obtain another mIPH distribution with a new initial distribution vector and smaller dimension: Let $X \sim \text{mIPH}(\boldsymbol{\pi}, \mathcal{T}, \mathcal{L})$ and condition on the value of X_l , $l \leq d$. The conditional density is

$$f_{X|X_l}(x | x_l) = \sum_{j=1}^p \frac{\pi_j \mathbf{e}_j^\top \exp(\mathbf{T}_l g_l^{-1}(x_l)) \mathbf{t}_l \lambda_l(x_l)}{\boldsymbol{\pi} \exp(\mathbf{T}_l g_l^{-1}(x_l)) \mathbf{t}_l \lambda_l(x_l)} \prod_{i \neq l} \mathbf{e}_j^\top \exp(\mathbf{T}_i g_i^{-1}(x_i)) \mathbf{t}_i \lambda_i(x_i).$$

That is,

$$(2.3) \quad X | X_l = x_l \sim \text{mIPH}(\boldsymbol{\alpha}, \mathcal{T} \setminus \mathbf{T}_l, \mathcal{L} \setminus \lambda_l),$$

with initial distribution vector

$$\boldsymbol{\alpha} = \left\{ \pi_j \times \frac{\mathbf{e}_j^\top \exp(\mathbf{T}_l g_l^{-1}(x_l)) \mathbf{t}_l \lambda_l(x_l)}{\boldsymbol{\pi} \exp(\mathbf{T}_l g_l^{-1}(x_l)) \mathbf{t}_l \lambda_l(x_l)} \right\}_{j \in E \setminus l}.$$

The same reasoning can be applied to obtain

$$(2.4) \quad X | X_l \geq x_l \sim \text{mIPH}(\boldsymbol{\nu}, \mathcal{T} \setminus \mathbf{T}_l, \mathcal{L} \setminus \lambda_l),$$

with

$$\boldsymbol{\nu} = \left\{ \pi_j \times \frac{\mathbf{e}_j^\top \exp(\mathbf{T}_l g_l^{-1}(x_l)) \mathbf{e}}{\boldsymbol{\pi} \exp(\mathbf{T}_l g_l^{-1}(x_l)) \mathbf{e}} \right\}_{j \in E \setminus l}.$$

Remark 2.1. One might be tempted to argue that Assumption (2.1) necessarily leads to positive dependence of the resulting random variables (in our case lifetimes). However, sharing the initial state is not sufficient to obtain positive dependence, as the different intensity matrices may introduce counter-effects. For instance, after starting in the same state we could have a very small expected holding time and direct absorption for one marginal, while the second has to pass through the entire state space before absorption happens, leading to a very large survival time. This behaviour could very well be reversed when starting in another (but common) state. Consequently, certain combinations of individual intensity matrices may give rise to negative dependence as well.

3. PARAMETER ESTIMATION FOR RIGHT-CENSORED DATA AND COVARIATE INFORMATION

In the following we introduce components needed to estimate the parameters of mIPH distributions, and we consider a general situation with covariate information and right-censored data.

3.1. Initial distribution vectors. Adapting an idea developed in [8], we apply the regression component to the initial distribution, i.e. we estimate a ‘personalised’ initial distribution vector as a function of covariates, which increases the flexibility of the model. To that end, we use multinomial logistic regressions, where we consider the initial probabilities as response variables that depend on covariate information found in $\mathbf{A}^{(m)\top} \in \mathbb{R}^g$, with g being the number of explanatory variables, $m = 1, \dots, n$, and regression coefficients in $\boldsymbol{\gamma} \in \mathbb{R}^{p \times g}$. Concretely, the initial distribution probabilities are then given as

$$\pi_k^{(m)} = \frac{\exp(\mathbf{A}^{(m)}\boldsymbol{\gamma}_k)}{\sum_{j=1}^p \exp(\mathbf{A}^{(m)}\boldsymbol{\gamma}_j)},$$

with $\boldsymbol{\gamma}_k \in \mathbb{R}^g$ for $k = 1, \dots, p$.

In every iteration of the expectation-maximisation (EM) algorithm to be described later, we use the conditional expectation of the number of times that the underlying process starts in a specific state as weights for the regression coefficients in $\boldsymbol{\gamma}$. We then solve the optimisation problem

$$\hat{\boldsymbol{\gamma}} = \arg \max_{\boldsymbol{\gamma}} \sum_{m=1}^n \sum_{k=1}^p \mathbb{E}(B_k^{(m)} \mid \Xi = \xi) \log(\pi_k^{(m)}(\mathbf{A}^{(m)}; \boldsymbol{\gamma}))$$

and set

$$(3.1) \quad \hat{\pi}_k^{(m)} = \pi_k^{(m)}(\mathbf{A}^{(m)}; \hat{\boldsymbol{\gamma}}) = \frac{\exp(\mathbf{A}^{(m)}\hat{\boldsymbol{\gamma}}_k)}{\sum_{j=1}^p \exp(\mathbf{A}^{(m)}\hat{\boldsymbol{\gamma}}_j)}$$

in every iteration. The initial distribution hence depends on covariate information. Recall that all marginal processes $\{J_t^{(i)}\}_{t \geq 0}$ are assumed to start in the same state (drawn from the initial distribution with probabilities (3.1)), but afterwards transit independently to other states according to their specific sub-intensity matrices (and the latter do not depend on covariate information). Their estimation is described next.

3.2. EM algorithm for right-censored data. Taking inspiration from Asmussen et al. [5] and Olsson [18], we now derive conditional expectations needed in the EM algorithm for mPH distributions, where absorption times are allowed to be right-censored. Since the eventually targeted mIPH distributions are transformed mPH distributions, after transformation of the data the E-Step and M-Step of the algorithm are the same as for the time-homogeneous case.

Let Ξ (respectively ξ) be the observed information of the sample at hand, at population level (respectively, at observation level). Let $\mathbf{Y} = (y_1^{(m)}, \dots, y_d^{(m)})$ be the collection of absorption times we want to fit, where $y_i^{(m)} \in \mathbb{R}_+^n$ for $i = 1, \dots, d$. We assume that the censoring mechanism is independent of the size of the random variables. The marginals $Y_i^{(m)} = \min(x_i^{(m)}, R_i^{(m)})$ follow PH($\boldsymbol{\pi}, \mathbf{T}_i$) distributions, where $R_i^{(m)}$ is a random censoring point for the m -th observation. The realisation of random right-censoring indicators can be found in $\boldsymbol{\Delta} = (\delta_1^{(m)}, \dots, \delta_d^{(m)})$, where elements $\delta_i^{(m)} \in \mathbb{R}_+^n$, $i = 1, \dots, d$, are equal to 1 if the absorption time $x_i^{(m)}$ is fully observed and 0 if $x_i^{(m)} \geq R_i^{(m)}$ is right-censored. With these assumptions, the derivation of conditional expectations needed to describe the incomplete likelihood of the sample, namely B_k , $Z_k^{(i)}$, $N_{ks}^{(i)}$ and $N_k^{(i)}$, for $k, s \in E$ and $i = 1, \dots, d$, is

analogous to the fully uncensored case (see [6]). The only difference from the fully observed case is that marginals may have right-censored absorption times. To see how this affects the expectation step of the EM algorithm, we give a detailed derivation of $\mathbb{E}(B_k \mid \Xi = \xi)$. For the m -th row of \mathbf{Y} , let $i_{un}^{(m)}$ denote the collection of indices of marginals that are uncensored and similarly $i_{rc}^{(m)}$ for right-censored marginals. Naturally $i_{un}^{(m)} + i_{rc}^{(m)} = d$. Then, the conditional expectation of the number of times that the process starts in state k is

$$\begin{aligned} \mathbb{E}(B_k \mid \Xi = \xi) &= \sum_{i=1}^d \sum_{m=1}^n \mathbb{E}(1\{J_0^{(i,m)} = k\} \mid \Xi = \xi) \\ &= d \times \sum_{m=1}^n \mathbb{P}(J_0^{(m)} = k \mid \Xi = \xi) \\ &= d \times \sum_{m=1}^n \frac{\mathbb{P}(J_0^{(m)} = k) \mathbb{P}(X_j \in dx_j^{(m)}, X_l \geq x_l^{(m)}; j \in i_{un}^{(m)}, l \in i_{rc}^{(m)} \mid J_0^{(m)} = k)}{\mathbb{P}(X_j \in dx_j^{(m)}, X_l \geq x_l^{(m)}; j \in i_{un}^{(m)}, l \in i_{rc}^{(m)})} \\ &= d \times \sum_{m=1}^n \frac{\pi_k^{(m)} \prod_{j \in i_{un}^{(m)}} \mathbf{e}_k^\top \exp(\mathbf{T}_j x_j^{(m)}) \mathbf{t}_j \prod_{l \in i_{rc}^{(m)}} \mathbf{e}_k^\top \exp(\mathbf{T}_l x_l^{(m)}) \mathbf{e}}{\sum_{s=1}^p \pi_s^{(m)} \prod_{j \in i_{un}^{(m)}} \mathbf{e}_s^\top \exp(\mathbf{T}_j x_j^{(m)}) \mathbf{t}_j \prod_{l \in i_{rc}^{(m)}} \mathbf{e}_s^\top \exp(\mathbf{T}_l x_l^{(m)}) \mathbf{e}}, \end{aligned}$$

where we see a mix of marginal densities and survival functions appearing in both the numerator and denominator. This expectation can also be expressed, using the Δ notation, as

$$\mathbb{E}(B_k \mid \Xi = \xi) = d \times \sum_{m=1}^n \frac{\pi_k^{(m)} \prod_{i=1}^d \left(\mathbf{e}_k^\top \exp(\mathbf{T}_i x_i^{(m)}) \mathbf{t}_i \right)^{\delta_i^{(m)}} \left(\mathbf{e}_k^\top \exp(\mathbf{T}_i x_i^{(m)}) \mathbf{e} \right)^{1-\delta_i^{(m)}}}{\sum_{j=1}^p \pi_j^{(m)} \prod_{i=1}^d \left(\mathbf{e}_j^\top \exp(\mathbf{T}_i x_i^{(m)}) \mathbf{t}_i \right)^{\delta_i^{(m)}} \left(\mathbf{e}_j^\top \exp(\mathbf{T}_i x_i^{(m)}) \mathbf{e} \right)^{1-\delta_i^{(m)}}}$$

and we shall use this style in the following. The other needed conditional expectations are obtained in a similar way, reading

$$\begin{aligned} \mathbb{E}(Z_k^{(i)} \mid \Xi = \xi) &= \sum_{m=1}^n \frac{\sum_{j=1}^p \pi_j^{(m)} \prod_{l \neq i} \left(\mathbf{e}_j^\top \exp(\mathbf{T}_l x_l^{(m)}) \mathbf{t}_l \right)^{\delta_l^{(m)}} \left(\mathbf{e}_j^\top \exp(\mathbf{T}_l x_l^{(m)}) \mathbf{e} \right)^{1-\delta_l^{(m)}}}{\sum_{j=1}^p \pi_j^{(m)} \prod_{i=1}^d \left(\mathbf{e}_j^\top \exp(\mathbf{T}_i x_i^{(m)}) \mathbf{t}_i \right)^{\delta_i^{(m)}} \left(\mathbf{e}_j^\top \exp(\mathbf{T}_i x_i^{(m)}) \mathbf{e} \right)^{1-\delta_i^{(m)}}} \times \\ &\quad \times \left[\mathbf{e}_k^\top \int_0^{x_i^{(m)}} \exp(\mathbf{T}_i(x_i^{(m)} - t)) \mathbf{t}_i \mathbf{e}_j^\top \exp(\mathbf{T}_i t) dt \mathbf{e}_k \right]^{\delta_i^{(m)}} \times \\ &\quad \times \left[\mathbf{e}_k^\top \int_0^{x_i^{(m)}} \exp(\mathbf{T}_i(x_i^{(m)} - t)) \mathbf{e} \mathbf{e}_j^\top \exp(\mathbf{T}_i t) dt \mathbf{e}_k \right]^{1-\delta_i^{(m)}}, \end{aligned}$$

$$\mathbb{E}(N_{ks}^{(i)} \mid \Xi = \xi) = t_{ks}^{(i)} \times \sum_{m=1}^n \frac{\sum_{j=1}^p \pi_j^{(m)} \prod_{l \neq i} \left(\mathbf{e}_j^\top \exp(\mathbf{T}_l x_l^{(m)}) \mathbf{t}_l \right)^{\delta_l^{(m)}} \left(\mathbf{e}_j^\top \exp(\mathbf{T}_l x_l^{(m)}) \mathbf{e} \right)^{1-\delta_l^{(m)}}}{\sum_{j=1}^p \pi_j^{(m)} \prod_{i=1}^d \left(\mathbf{e}_j^\top \exp(\mathbf{T}_i x_i^{(m)}) \mathbf{t}_i \right)^{\delta_i^{(m)}} \left(\mathbf{e}_j^\top \exp(\mathbf{T}_i x_i^{(m)}) \mathbf{e} \right)^{1-\delta_i^{(m)}}} \times$$

$$\begin{aligned} & \times \left[\mathbf{e}_s^\top \int_0^{x_i^{(m)}} \exp(\mathbf{T}_i(x_i^{(m)} - t)) \mathbf{t}_i \mathbf{e}_j^\top \exp(\mathbf{T}_i t) dt \mathbf{e}_k \right]^{\delta_i^{(m)}} \times \\ & \times \left[\mathbf{e}_s^\top \int_0^{x_i^{(m)}} \exp(\mathbf{T}_i(x_i^{(m)} - t)) \mathbf{e} \mathbf{e}_j^\top \exp(\mathbf{T}_i t) dt \mathbf{e}_k \right]^{1-\delta_i^{(m)}}, \end{aligned}$$

and finally

$$\begin{aligned} \mathbb{E}(N_k^{(i)} \mid \Xi = \xi) &= t_k^{(i)} \times \sum_{m=1}^n \sum_{j=1}^p \pi_j^{(m)} \mathbf{e}_j^\top \exp(\mathbf{T}_i x_i^{(m)}) \mathbf{e}_k \delta_i^{(m)} \times \\ & \times \frac{\prod_{l \neq i} \left(\mathbf{e}_j^\top \exp(\mathbf{T}_l x_l^{(m)}) \mathbf{t}_l \right)^{\delta_l^{(m)}} \left(\mathbf{e}_j^\top \exp(\mathbf{T}_l x_l^{(m)}) \mathbf{e} \right)^{1-\delta_l^{(m)}}}{\sum_{j=1}^p \pi_j^{(m)} \prod_{i=1}^d \left(\mathbf{e}_j^\top \exp(\mathbf{T}_i x_i^{(m)}) \mathbf{t}_i \right)^{\delta_i^{(m)}} \left(\mathbf{e}_j^\top \exp(\mathbf{T}_i x_i^{(m)}) \mathbf{e} \right)^{1-\delta_i^{(m)}}}. \end{aligned}$$

As described earlier, in order to perform the multinomial logistic regression we need to consider the information carried by $\mathbb{E}(B_k \mid \Xi = \xi)$ separately. For a row of observations m , the expected number of times that the marginal jump processes start in state k is

$$\mathbb{E}(B_k^{(m)} \mid \Xi = \xi) = d \times \frac{\pi_k^{(m)} \prod_{i=1}^d \left(\mathbf{e}_k^\top \exp(\mathbf{T}_i x_i^{(m)}) \mathbf{t}_i \right)^{\delta_i^{(m)}} \left(\mathbf{e}_k^\top \exp(\mathbf{T}_i x_i^{(m)}) \mathbf{e} \right)^{1-\delta_i^{(m)}}}{\sum_{j=1}^p \pi_j^{(m)} \prod_{i=1}^d \left(\mathbf{e}_j^\top \exp(\mathbf{T}_i x_i^{(m)}) \mathbf{t}_i \right)^{\delta_i^{(m)}} \left(\mathbf{e}_j^\top \exp(\mathbf{T}_i x_i^{(m)}) \mathbf{e} \right)^{1-\delta_i^{(m)}}},$$

which for $k = 1, \dots, p$ are used as weights for the multinomial regression.

Consider now a multivariate sample of right-censored absorption times $\mathbf{Y} = (y_1^{(m)}, \dots, y_d^{(m)})$, which we assume to originate from $Y^{(m)} \sim \text{mIPH}(\boldsymbol{\pi}^{(m)}, \mathcal{T}, \mathcal{L})$. The associated inhomogeneity functions depend on parameters β_i , $i = 1, \dots, d$, and the right-censoring indicators are collected in $\boldsymbol{\Delta}$. The resulting EM algorithm with covariate information is depicted in Algorithm 1. As in Albrecher et al. [3], we firstly take care of time-inhomogeneity. Using the relation $g_i^{-1}(y_i^{(m)}) = \int_0^{y_i^{(m)}} \lambda_i(u; \beta_i) du$, $i = 1, \dots, d$, we obtain a time-homogeneous random sample, for which we know how to evaluate conditional expectations of sufficient statistics. Using these expectations (as given above), we estimate the marginal sub-intensity matrices, while the initial distribution vectors are predicted by multinomial logistic regressions. Once we have estimated both, we need to find optimal inhomogeneity parameters β_i , $i = 1, \dots, d$, that maximise the joint likelihood of the time-inhomogeneous sample. Concretely, we solve

$$\hat{\boldsymbol{\beta}} = \arg \max_{\boldsymbol{\beta}} \sum_{m=1}^n \log \left(\sum_{j=1}^p \hat{\pi}_j^{(m)} \prod_{i=1}^d \left(\mathbf{e}_j^\top \exp(\hat{\mathbf{T}}_i x_i^{(m)}) \hat{\mathbf{t}}_i \lambda_i(y_i^{(m)}, \beta_i) \right)^{\delta_i^{(m)}} \left(\mathbf{e}_j^\top \exp(\hat{\mathbf{T}}_i x_i^{(m)}) \mathbf{e} \right)^{1-\delta_i^{(m)}} \right),$$

where $x_i^{(m)} = g_i^{-1}(y_i^{(m)})$. We repeat the procedure until a stopping rule is satisfied, and finally obtain the estimated distribution $\text{mIPH}(\hat{\boldsymbol{\pi}}, \hat{\mathcal{T}}, \hat{\mathcal{L}})$. Here $\hat{\boldsymbol{\pi}}$ is a matrix, where each row is a distribution vector $\hat{\boldsymbol{\pi}}^{(m)}$, which is shared by marginals with the same covariates.

Algorithm 1 *Adapted expectation maximisation for mIPH distributions*

Input: Absorption times $\mathbf{Y} \in \mathbb{R}_+^{n \times d}$, right-censoring indicators $\mathbf{\Delta} \in \mathbb{R}^{n \times d}$ and arbitrary initial parameters for $(\boldsymbol{\pi}, \mathcal{T}, \mathcal{L})$.

- 1) For each marginal, transform the data in $x_i^{(m)} = g_i^{-1}(y_i^{(m)}; \beta_i)$, $i = 1, 2, \dots, d$ and $m = 1, 2, \dots, n$
- 2) E-step: Calculate

$$\begin{aligned} \mathbb{E}(B_k^{(m)} \mid \Xi = \xi) \quad & k = 1, \dots, p, \quad m = 1, \dots, n \\ \mathbb{E}(Z_k^{(i)} \mid \Xi = \xi) \quad & k = 1, \dots, p, \quad i = 1, \dots, d \\ \mathbb{E}(N_{ks}^{(i)} \mid \Xi = \xi) \quad & k, s = 1, \dots, p, \quad i = 1, \dots, d \\ \mathbb{E}(N_k^{(i)} \mid \Xi = \xi) \quad & k = 1, \dots, p, \quad i = 1, \dots, d \end{aligned}$$

- 3) R-step: Perform a multinomial regression with weights given by $\mathbb{E}(B_k^{(m)} \mid \Xi = \xi)$ and predict $\hat{\pi}_k^{(m)}$ for $k = 1, \dots, p$ and $m = 1, \dots, n$.
- 4) M-step: Let

$$\begin{aligned} \hat{t}_{ks}^{(i)} &= \frac{\mathbb{E}(N_{ks}^{(i)} \mid \Xi = \xi)}{\mathbb{E}(Z_k^{(i)} \mid \Xi = \xi)}, \quad k, s = 1, \dots, p, \quad i = 1, \dots, d \\ \hat{t}_k^{(i)} &= \frac{\mathbb{E}(N_k^{(i)} \mid \Xi = \xi)}{\mathbb{E}(Z_k^{(i)} \mid \Xi = \xi)} \quad k = 1, \dots, p, \quad i = 1, \dots, d \\ \hat{t}_{kk}^{(i)} &= - \sum_{s \neq k} \hat{t}_{ks}^{(i)} - \hat{t}_k^{(i)} \quad k, s = 1, \dots, p, \quad i = 1, \dots, d \end{aligned}$$

$$\text{Let } \hat{\boldsymbol{\pi}} = (\hat{\pi}_1^{(m)}, \dots, \hat{\pi}_p^{(m)}), \quad \hat{\mathbf{T}}_i = \{\hat{t}_{ks}^{(i)}\}_{k,s=1,2,\dots,p}, \quad \text{and} \quad \hat{\mathbf{t}}_i = \begin{pmatrix} \hat{t}_1^{(i)} \\ \vdots \\ \hat{t}_p^{(i)} \end{pmatrix}.$$

- 5) I-step: Compute

$$\begin{aligned} \hat{\boldsymbol{\beta}} &= \arg \max_{\boldsymbol{\beta}} \sum_{m=1}^n \log \left(f_Y(y^{(m)}; \hat{\boldsymbol{\pi}}, \hat{\mathcal{T}}, \boldsymbol{\beta}, \mathbf{\Delta}) \right) \\ &= \arg \max_{\boldsymbol{\beta}} \sum_{m=1}^n \log \left(\sum_{j=1}^p \hat{\pi}_j^{(m)} \prod_{i=1}^d \left(\mathbf{e}_j^\top \exp(\hat{\mathbf{T}}_i x_i^{(m)}) \hat{\mathbf{t}}_i \lambda_i(y_i^{(m)}, \beta_i) \right)^{\delta_i^{(m)}} \left(\mathbf{e}_j^\top \exp(\hat{\mathbf{T}}_i x_i^{(m)}) \mathbf{e} \right)^{1-\delta_i^{(m)}} \right) \end{aligned}$$

- 6) Assign $\boldsymbol{\pi} = \hat{\boldsymbol{\pi}}$, $\mathbf{T}_i = \hat{\mathbf{T}}_i$ and $\beta_i = \hat{\beta}_i$ then repeat from Step 1 until a stopping rule is satisfied.

Output: Fitted representations $(\hat{\boldsymbol{\pi}}, \hat{\mathcal{T}}, \hat{\mathcal{L}})$, for $m = 1, \dots, n$.

In contrast to copula-based methods, a particular advantage of this approach is that one does not separate the estimation of marginals and multivariate parameters.

4. MODELLING JOINT EXCESS LIFETIMES OF COUPLES

In this section we present an application of Algorithm 1 to the well-known data set of joint lives used in [12]. In addition to survival times, this data set provides information on individuals' ages at issuance of an insurance policy. This leads to left-truncated data in this particular case, and one might indeed consider the different entry ages with a left-truncated likelihood in the estimation process, which is, however, quite inefficient. Instead, we propose here to use entry age as a covariate information and use multinomial logistic regression to deal with the different ages at issuance. Initial distribution vectors obtained via regression will then incorporate the fact that an old couple is expected to survive less long than a young one, and that the bereavement effect may be different for different age dynamics in a couple. In PH terms, when using an acyclical distribution, the older the couple the larger the starting probabilities should be for states closer to the absorbing state, so that fewer states will be visited until absorption. Passing through fewer states translates into less time spent in the state-space before exiting, which results in smaller remaining lifetimes.

4.1. Description of the data set. The data set at hand provides information about 14947 insurance products on joint lives, which were observed from December 29, 1988 until December 31, 1993. We consider January 1, 1994 as the right censoring limit. For the purpose of this paper, we only consider birthdays, sexes (and potential death dates) of policyholders, given that we are only interested in mortality, i.e. we do not make use of the monetary details of each contract.

After removing same-sex couples and multiple entries (due to several contracts of the same couple), we compute the excess lifetime that any person lived from the start of the observation period until the right-censoring date 01.01.1994, given that they are at least 40 years old at the issuance of the policy. Doing so leads to 8834 different joint excess survival times, with 155 cases where both individuals died, 1057 where only one individual died and 7622 where neither died. Consequently, less than 2% of joint excess survival times are fully observed. Among the couples where only one person died, in 820 of them this was the man, and in the complementary 237 cases the woman died. Hereafter, we refer to the start of the observation period as the “issuance of the policy”, although the actual issue date may be older than 29.12.1988.

To prepare the data for the multinomial regression, we construct the covariate matrix $\mathbf{A} = (\mathbf{1} \text{ } age_x \text{ } age_y \text{ } interact)$, $\mathbf{A} \in \mathbb{R}^{n \times 4}$. The column vector age_x is the collection of all ages of men, at issuance of a policy, while age_y contains all ages of women. We also consider an interaction term in *interact*, which gathers element-wise multiplication of ages in a couple. Finally, to perform multinomial regressions via neural networks (R package *nnet*), we divide the data by 100, such that an absorption time of 0.01 given by estimated distributions actually corresponds to 1 year.

4.2. Fitting the mIPH distribution: Marginal behaviour. We assume that the remaining lifetimes in a couple, after issue of an insurance policy, follow mIPH distributions. We use information previously discussed as covariates to link starting probabilities to ages of individuals in couples, in order to reflect different ageing dynamics in our model.

The distribution with covariate information we work with is given by marginal Matrix-Gompertz distributions with general Coxian sub-intensity matrices of dimension $p = 10$ (cf. [2]). Let $Y_i^{(m)} = \log(\beta_i X_i^{(m)} + 1)/\beta_i$, be the marginal IPH distributions, with $X_i^{(m)} \sim \text{PH}(\boldsymbol{\pi}^{(m)}, \mathbf{T}_i)$ and $\beta_i > 0$, where $i = 1$ corresponds to men and $i = 2$ to women. According to the dependence structure defined in (2.1), after both underlying processes $\{J_t^{(1)}\}_{t \geq 0}$ and $\{J_t^{(2)}\}_{t \geq 0}$ start in the same state they evolve independently until absorption. With a general Coxian sub-intensity matrix, each marginal jump process is only allowed to transit to the next state or directly to the absorption state. This stochastic structure has a nice interpretation in terms of ageing. Indeed, we can think of forward transitions as natural ageing steps, given that each time the process jumps to a certain state, the time of absorption gets closer. Moreover, premature exits can be interpreted as deaths due to causes not related to ageing. Indeed, given that exit rates are positive in each state, the absorption of a process may be caused by a transition to State $p + 1$ from a state smaller than p . Finally, granting the underlying processes to start in different states allows heterogeneity of health statuses for individuals of the same age (this philosophy was already underlying the construction in [15], but with the present inhomogeneity, much fewer states are needed to describe the data satisfactorily).

Algorithm 1 is now applied for 1000 iterations. In principle, this estimation procedure provides $n = 8834$ different initial distribution vectors, one for each couple depending on the ages at issuance. Figure 4.1 depicts the age combinations in the data, with a majority of couples having a small age difference at policy issuance. For illustration purposes, we

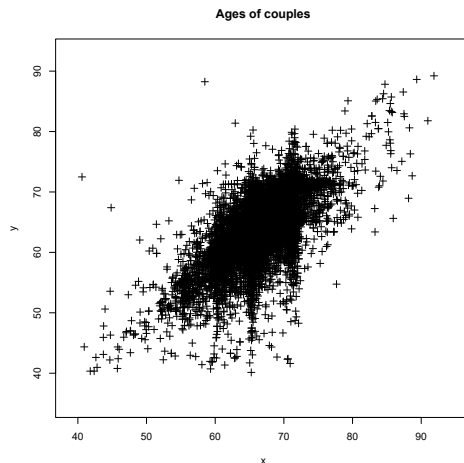


FIGURE 4.1. Ages at issuance of policies, for all couples.

depict below the estimated initial distributions for four different age combinations (age man, age woman): (63,63), (68,63), (63,68) and (73,63), which were chosen arbitrarily, but to represent different ageing dynamics at issuance of the policy.

Let $\mathbf{Y}^c = (Y_1^c, Y_2^c) \sim \text{mIPH}(\hat{\boldsymbol{\pi}}^c, \hat{\mathcal{T}}, \hat{\mathcal{L}})$ denote the bivariate distribution of excess lifetimes for these four couples, where $c = 1, 2, 3, 4$, $\hat{\mathcal{T}} = \{\hat{\mathbf{T}}_1, \hat{\mathbf{T}}_2\}$ and $\hat{\mathcal{L}} = \{\lambda_1(\cdot, \hat{\beta}_1), \lambda_2(\cdot, \hat{\beta}_2)\}$. The

common estimated sex-specific sub-intensity matrices are

$$(4.1) \quad \hat{\mathbf{T}}_1 = \begin{pmatrix} -0.049 & 1.7/10^7 & 0 & 0 & 0 & 0 & 0 & 0 & 0 & 0 \\ 0 & -3.662 & 2.877 & 0 & 0 & 0 & 0 & 0 & 0 & 0 \\ 0 & 0 & -1.8/10^7 & 1.8/10^7 & 0 & 0 & 0 & 0 & 0 & 0 \\ 0 & 0 & 0 & -1.9/10^4 & 1.9/10^4 & 0 & 0 & 0 & 0 & 0 \\ 0 & 0 & 0 & 0 & -0.611 & 0.611 & 0 & 0 & 0 & 0 \\ 0 & 0 & 0 & 0 & 0 & -0.002 & 0.002 & 0 & 0 & 0 \\ 0 & 0 & 0 & 0 & 0 & 0 & -9.778 & 5.73 & 0 & 0 \\ 0 & 0 & 0 & 0 & 0 & 0 & 0 & -0.36 & 0.225 & 0 \\ 0 & 0 & 0 & 0 & 0 & 0 & 0 & 0 & -1.852 & 1.099 \\ 0 & 0 & 0 & 0 & 0 & 0 & 0 & 0 & 0 & -0.023 \end{pmatrix}$$

for men and

$$(4.2) \quad \hat{\mathbf{T}}_2 = \begin{pmatrix} -0.196 & 0.196 & 0 & 0 & 0 & 0 & 0 & 0 & 0 & 0 \\ 0 & -0.291 & 0.291 & 0 & 0 & 0 & 0 & 0 & 0 & 0 \\ 0 & 0 & -0.763 & 0.763 & 0 & 0 & 0 & 0 & 0 & 0 \\ 0 & 0 & 0 & -2.8/10^8 & 2.8/10^8 & 0 & 0 & 0 & 0 & 0 \\ 0 & 0 & 0 & 0 & -0.001 & 0.001 & 0 & 0 & 0 & 0 \\ 0 & 0 & 0 & 0 & 0 & -0.003 & 0.003 & 0 & 0 & 0 \\ 0 & 0 & 0 & 0 & 0 & 0 & -3.182 & 1.165 & 0 & 0 \\ 0 & 0 & 0 & 0 & 0 & 0 & 0 & -0.172 & 2/10^7 & 0 \\ 0 & 0 & 0 & 0 & 0 & 0 & 0 & 0 & -0.008 & 2.3/10^{10} \\ 0 & 0 & 0 & 0 & 0 & 0 & 0 & 0 & 0 & -3/10^6 \end{pmatrix}$$

for women. The optimal inhomogeneity parameters are $\hat{\beta}_1 = 43.101$ and $\hat{\beta}_2 = 47.474$, and Table 4.1 presents the estimated coefficients of the last multinomial regression performed in Algorithm 1. Besides States 8 and 9, all other coefficients in $\hat{\gamma}$ are significant. Initial distribution vector estimates for these four couples are

$$\begin{aligned} \hat{\pi}^1 &= (0.0526 \ 0.0734 \ 0.0448 \ 0.0886 \ 0.4065 \ 0.0330 \ 0.0326 \ 0.0569 \ 0.1077 \ 0.1039), \\ \hat{\pi}^2 &= (0.0356 \ 0.0313 \ 0.0297 \ 0.0398 \ 0.2805 \ 0.0476 \ 0.0396 \ 0.0384 \ 0.2472 \ 0.2102), \\ \hat{\pi}^3 &= (0.0285 \ 0.0242 \ 0.0114 \ 0.1625 \ 0.4399 \ 0.0419 \ 0.0304 \ 0.1282 \ 0.0819 \ 0.0510), \\ \hat{\pi}^4 &= (0.0172 \ 0.0095 \ 0.0140 \ 0.0127 \ 0.1378 \ 0.0489 \ 0.0343 \ 0.0184 \ 0.4041 \ 0.3030). \end{aligned}$$

At first glance, it might seem odd that survival times of spouses with large age difference start in the same state of the distribution, but personalised starting probabilities and sex-specific transition intensities account for this. For example, consider Couple 4. If both excess survival times start in State 1, we see that the man's underlying jump process is much more likely to reach the absorbing state directly from State 1, while the woman's will at least advance to State 7 before absorption becomes possible. Thus, marginal intensities mixed with age-dependent initial distribution vectors compensate the initialisation in a shared state. In Figure 4.2 we depict the resulting marginal densities of the fitted remaining lifetime distributions for each of the four couples. As expected, the densities for women (solid black lines) allocate more mass to larger values than the male counterpart, and for

p	Intercept	age_x	age_y	$age_x \cdot age_y$
2	-20.963*** (7.157)	43.733*** (11.238)	43.021*** (12.400)	-84.049*** (19.311)
3	24.826*** (6.677)	-24.630** (10.476)	-39.256*** (11.639)	38.453** (18.073)
4	-51.036*** (9.894)	57.442*** (15.348)	90.062*** (15.820)	-104.233*** (24.374)
5	-42.469*** (6.873)	56.804*** (10.638)	70.273*** (11.443)	-89.556*** (17.559)
6	14.850* (8.004)	-41.377*** (12.150)	-39.438*** (12.824)	89.687*** (19.317)
7	54.157*** (6.617)	-97.618*** (10.263)	-98.445*** (11.010)	173.553*** (16.817)
8	-14.363 (9.419)	-5.608 (14.387)	22.990 (14.885)	8.794 (22.584)
9	-11.589 (7.224)	12.732 (11.046)	-4.892 (11.889)	18.559 (18.050)
10	21.474*** (6.504)	-31.068*** (10.054)	-54.907*** (10.892)	84.080*** (16.670)

TABLE 4.1. Coefficients of multinomial regression with associated standard errors in brackets. For a two sided statistical test symbols * * *, ** and * correspond to significance levels of 1%, 5% and 10% respectively.

older individuals there is more probability mass for shorter survival times. Comparing Couples 1 and 4, we see that the density of the 63-year-old man has a major mode at $x = 22$, while for the 73-year-old man, the major mode is at $x = 17$. Note that despite the fact that the women in Couples 1 and 4 are of comparable age, their densities have substantially different modes. This is due to the fact that the estimation of the marginal distributions is not separated from the estimation of the joint distributions, and the age of their spouse at the time of policy issuance evidently plays an important role for the distribution of the remaining lifetime, seen at the time of policy issuance.

The multimodality we observe in all marginal densities may be due to having different cohorts in the data. We decided not to manipulate the data set further, in order to avoid restricting our analysis to specific couples. Although spouses with small age difference can be thought of as belonging to the same cohort, we would also need to restrain the ages at issuance to instances where enough data points are available for a meaningful estimation

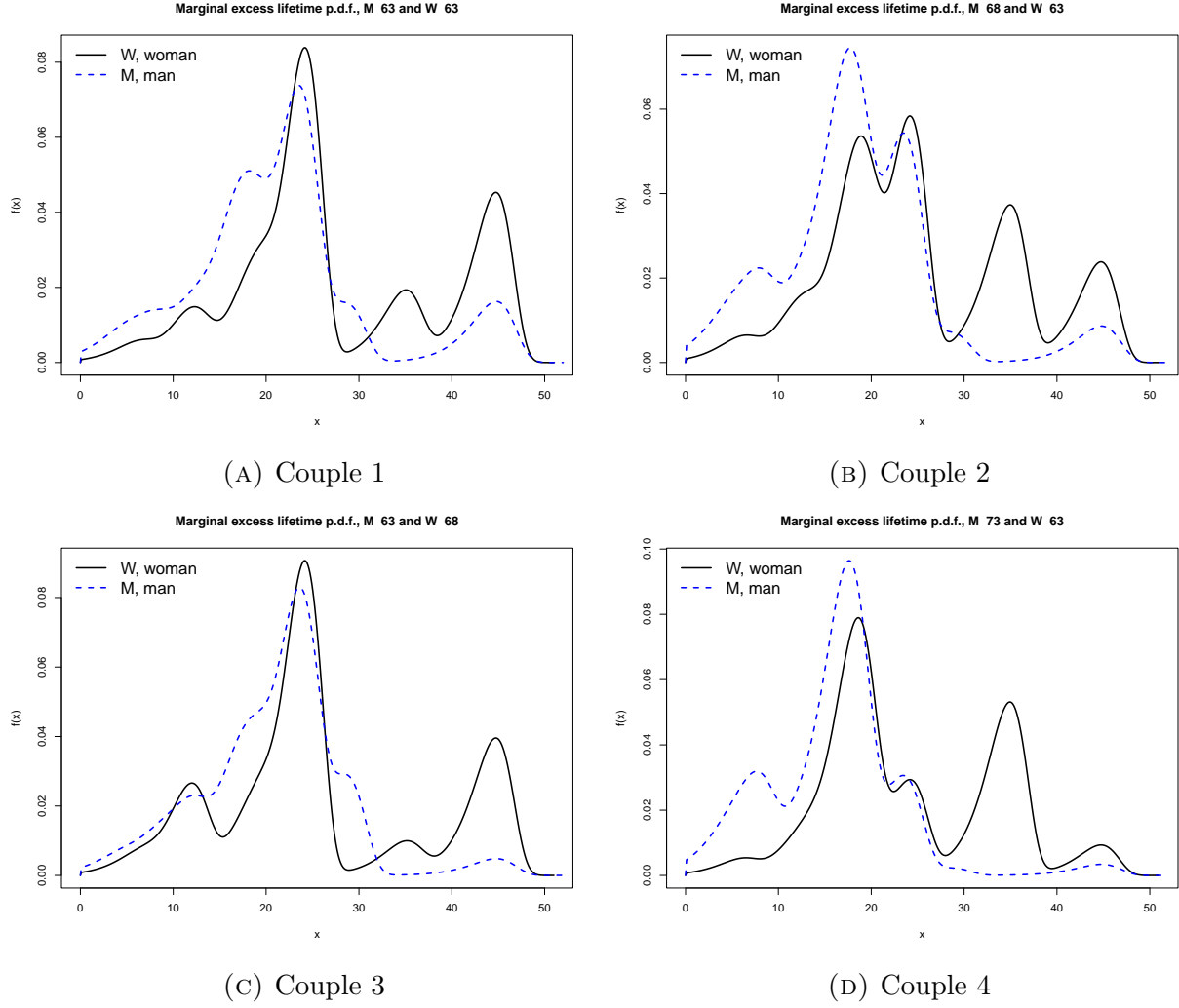


FIGURE 4.2. Marginal densities of remaining life times (in years).

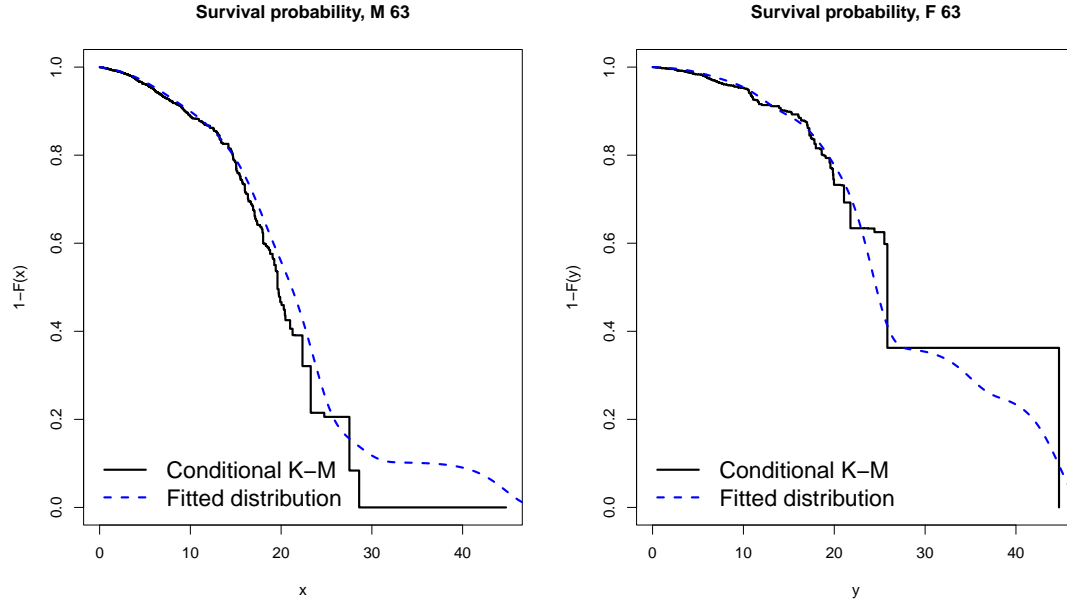
procedure (in particular uncensored data points). Doing so would lead to analysing only couples where both spouses are aged around 65 years old.

To assess the precision of our estimated marginals $Y_i^c \sim \text{IPH}(\hat{\boldsymbol{\pi}}, \hat{\boldsymbol{T}}_i, \hat{\beta}_i)$, $i = 1, 2$ and $c = 1, 2, 3, 4$, we use the conditional Kaplan-Meier (K-M in the following) estimator, also known as Beran estimator. For a sample X_1, X_2, \dots, X_n and covariate matrix \mathbf{A} , the conditional K-M estimator we use is

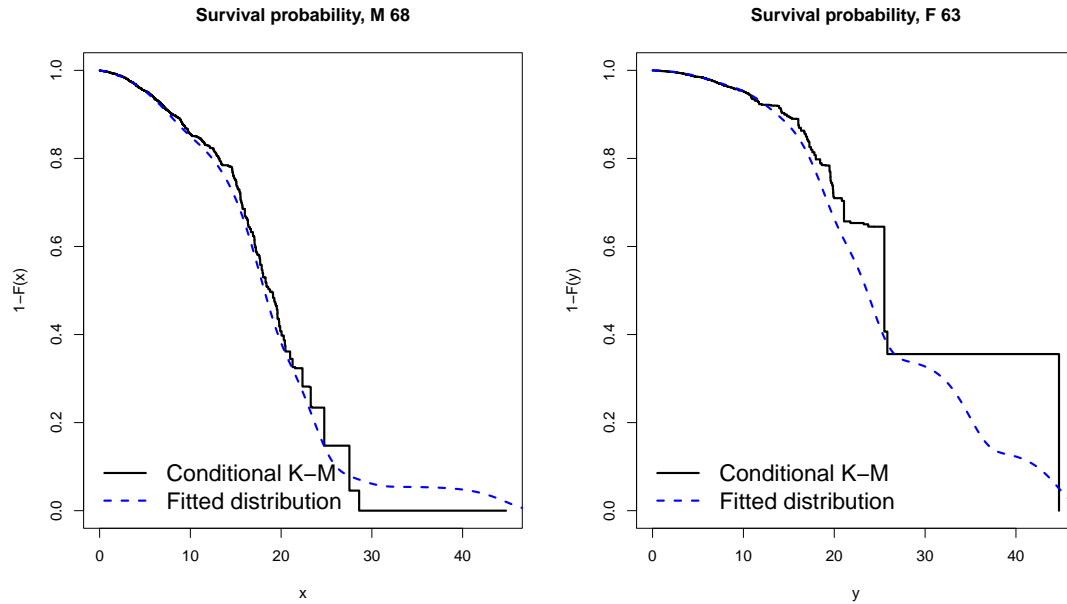
$$(4.3) \quad \hat{\mathbb{P}}(X \leq t \mid \mathbf{A} = \mathbf{a}) = \hat{F}_X(t \mid \mathbf{a}) = 1 - \prod_{i: X_{i:n} \leq t} \left(1 - \frac{\delta_{i:n} K\left(\frac{\mathbf{a} - \mathbf{A}_{i:n}}{b_n}\right)}{\sum_{j=i}^n K\left(\frac{\mathbf{a} - \mathbf{A}_{j:n}}{b_n}\right)} \right),$$

where $X_{i:n}$ are order statistics of the sample, $\delta_{i:n}$ the respective right-censoring indicators, $K(\cdot)$ is a kernel function and b_n is a band sequence. In our instance, the kernel function is a multivariate Gaussian density and $b_n = 0.001$. For more details on the conditional K-M estimator we refer the reader to Dabrowska [10]. Figures 4.3 and 4.4 compare the

survival probabilities obtained by the conditional K-M estimators with the one of the fitted distributions. One sees that in all cases the fit is in fact quite satisfactory.

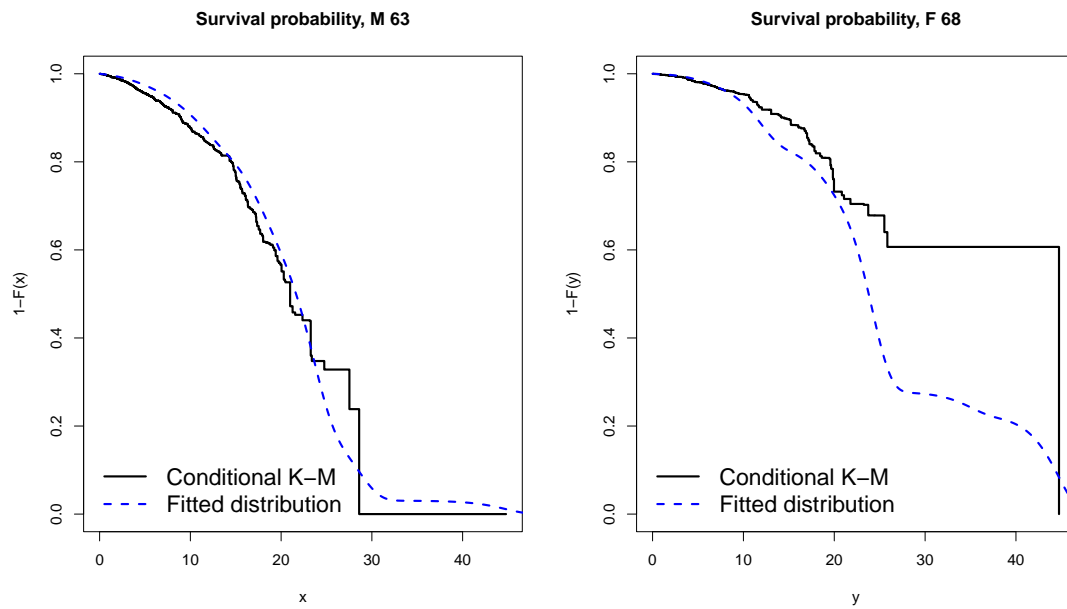


(A) Couple 1

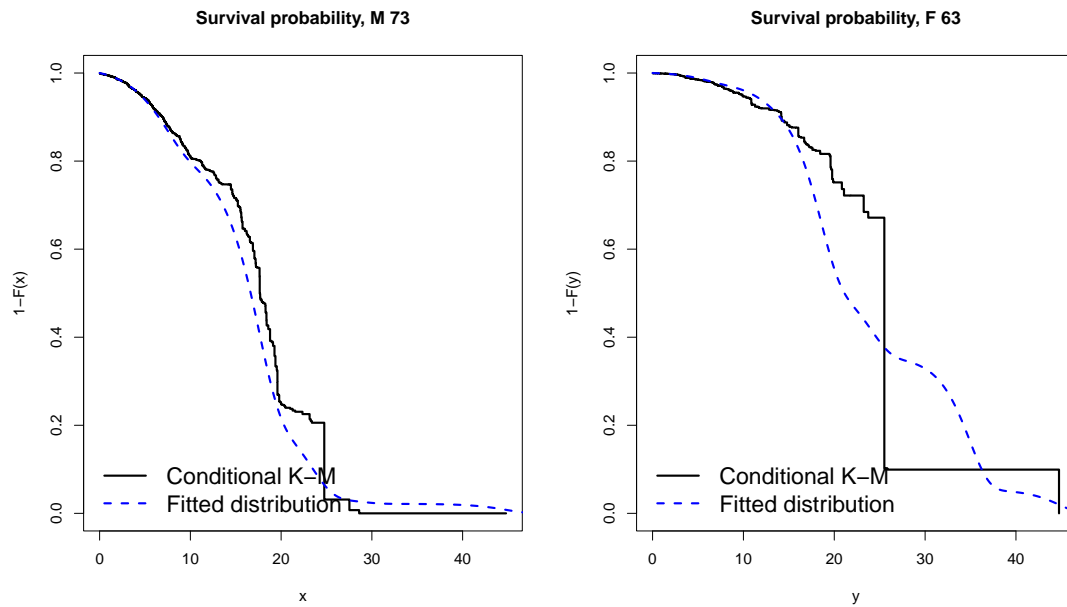


(B) Couple 2

FIGURE 4.3. Conditional K-M estimators vs the fitted distribution, Couples 1 and 2.



(A) Couple 3



(B) Couple 4

FIGURE 4.4. Conditional K-M estimators vs the fitted distribution, Couple 3 and 4.

4.3. Joint behaviour. Let us now consider the resulting bivariate densities. In Figure 4.5 we find the bivariate densities for the four specified couples. The joint density of Couple 1 shows that large differences in their survival times are quite unlikely (the vast majority of the joint mass being located close the identity line). Also, the most likely survival times

are close to 23 years. There is also a considerable probability mass above the identity line, where the woman survives longer than the man. For instance, we have $\bar{F}_{Y^1}(12, 30) = 32\%$ while $\bar{F}_{Y^2}(30, 12) = 11.79\%$.

For Couple 2 the situation is different (top right panel of Figure 4.5): with the man being already 68 years and the woman being 63 years old, the remaining lifetimes are shorter, with the major mode of the joint distribution being located near $(x, y) = (23, 24)$, the second largest close to $(x, y) = (17, 35)$ and the next ones in the neighbourhood of $(x, y) = (17, 19)$ and $(x, y) = (9, 19)$, respectively. There is now a much higher probability for the husband to die sooner.

The joint density for Couple 3 resembles the one of Couple 1, with survival times beyond 40 years being more unlikely. Despite the man being at the same age at issuance, there is a larger probability for the woman to survive the man than for Couple 1, with a spike near $(x, y) = (29, 45)$.

Finally, the joint density of Couple 4 is close to the one of Couple 2. The spike around $(x, y) = (17, 35)$ is more pronounced than the analogue of Couple 2, while the spike close to $(x, y) = (23, 24)$ is less important than its counterpart in Couple 2.

One may be tempted to conclude from these four distributions that for the same age, having a younger partner leads to longer survival times, which would signal that the bereavement effect is weaker when spouses have larger differences in age at issuance of a policy.

4.4. Dependence measures. Let us now explore some dependence measures for these four exemplary couples. In addition to Kendall's tau and Spearman's rho, we also consider three measures of time-dependent association, which were analysed in Luciano et al. [16]. The mIPH distributions we consider all have the same copula as the corresponding mPH distributions with equal representation, since matrix-Gompertz distributions are monotone increasing transformations of PH distributions. At the same time, for the mPH class we have explicit expressions for Kendall's tau and Spearman's rho. The pairwise Kendall's tau of marginals X_k and X_l is

$$\tau_{X_k, X_l} = 4 \sum_{i=1}^p \sum_{j=1}^p \pi_i \pi_j (\mathbf{e}_i^\top \otimes \mathbf{e}_j^\top) [-\mathbf{T}_k \oplus \mathbf{T}_k]^{-1} (\mathbf{e} \otimes \mathbf{t}_k) (\mathbf{e}_i^\top \otimes \mathbf{e}_j^\top) [-\mathbf{T}_l \oplus \mathbf{T}_l]^{-1} (\mathbf{e} \otimes \mathbf{t}_l) - 1,$$

while Spearman's rank correlation is given as

$$\rho_{X_k, X_l}^S = 12 \sum_{j=1}^p \pi_j \left(1 - (\boldsymbol{\pi} \otimes \mathbf{e}_j^\top) [-\mathbf{T}_k \oplus \mathbf{T}_k]^{-1} (\mathbf{e} \otimes \mathbf{t}_k) \right) \left(1 - (\boldsymbol{\pi} \otimes \mathbf{e}_j^\top) [-\mathbf{T}_l \oplus \mathbf{T}_l]^{-1} (\mathbf{e} \otimes \mathbf{t}_l) \right) - 3,$$

cf. [6]. Calculating these quantities for the four specified couples, one obtains

$$\begin{aligned} \tau_{Y_1^1, Y_2^1} &= 0.3104, & \tau_{Y_1^2, Y_2^2} &= 0.2562, & \tau_{Y_1^3, Y_2^3} &= 0.4367, & \tau_{Y_1^4, Y_2^4} &= 0.2139, \\ \rho_{Y_1^1, Y_2^1}^S &= 0.4526, & \rho_{Y_1^2, Y_2^2}^S &= 0.3938, & \rho_{Y_1^3, Y_2^3}^S &= 0.6144, & \rho_{Y_1^4, Y_2^4}^S &= 0.3381. \end{aligned}$$

All couples manifest positive concordance, which on top of Figure 4.5 is additional evidence that the lifetimes of individuals in a couple are correlated. We find the strongest concordance in couples where women are older than their husbands. Concretely, Couple 3 has the highest Kendall's tau and Spearman's rho values, followed by Couple 1. Couple 2 and Couple 4 have lower, and similar, corresponding values.

As a first measure of time-dependent association, we consider in Figure 4.6

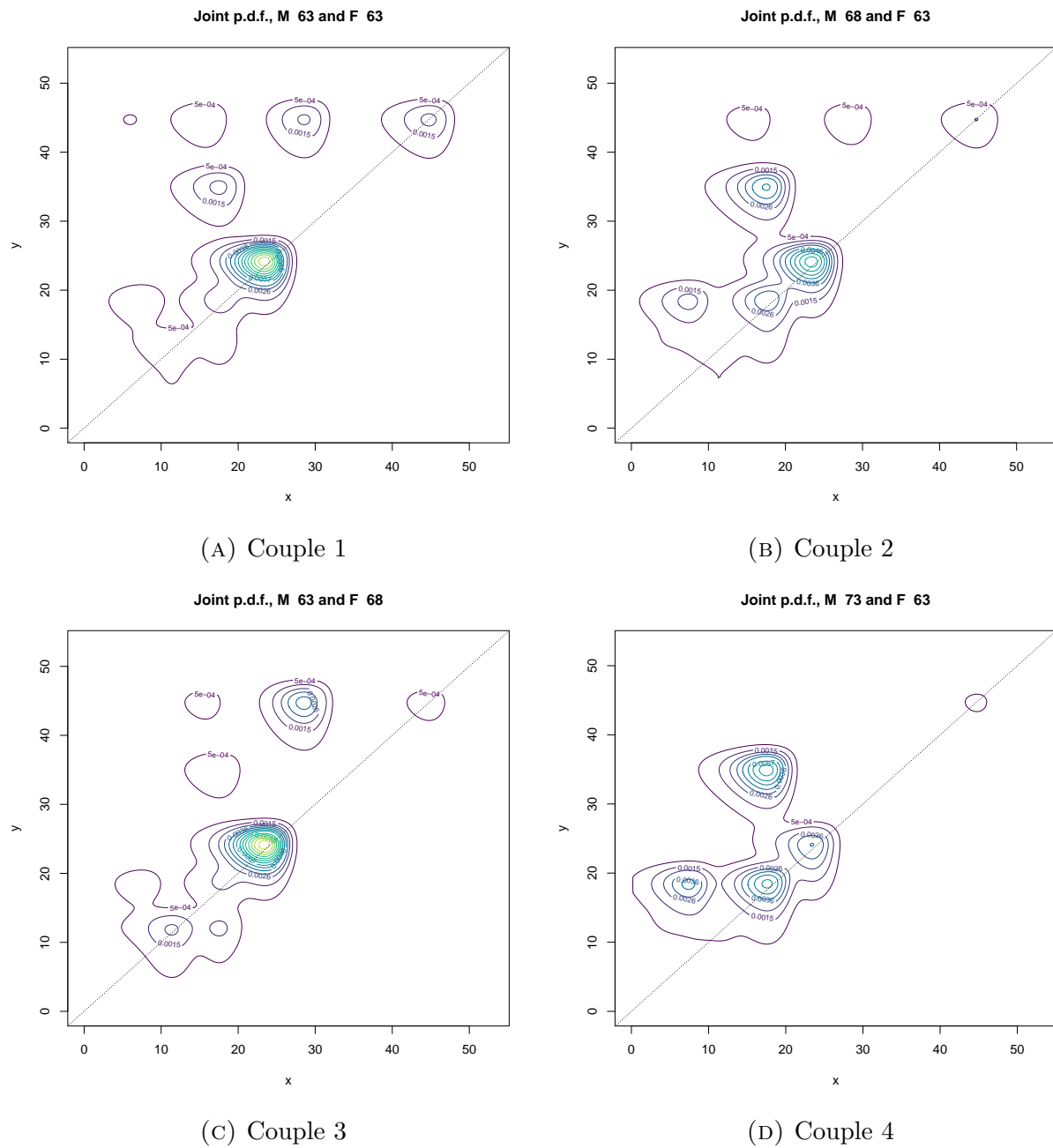
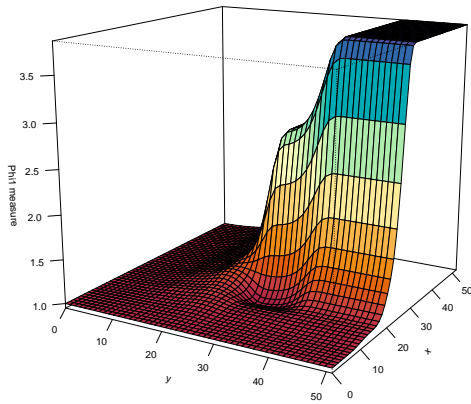


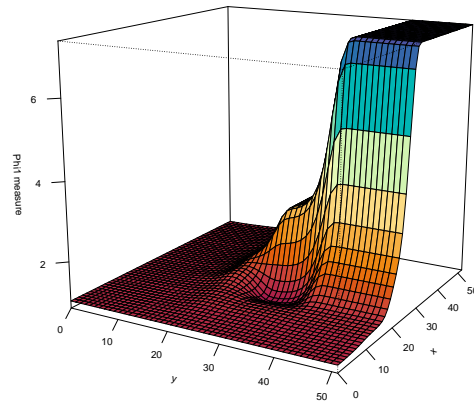
FIGURE 4.5. Contour plots of the bivariate lifetime densities for the four couples

$$\Psi_1(x, y) = S(x, y) / (S_{Y_1}(x)S_{Y_2}(y)).$$

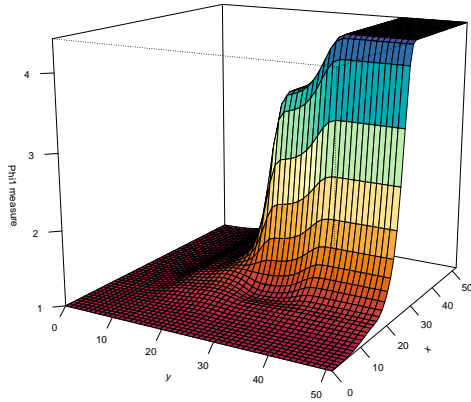
Most of the resulting values are greater than 1, indicating positive dependence. However, for values of y close to 30, Couples 1, 2 and 3 exhibit $\Psi_1(x, y) < 1$. This suggests negative dependence for remaining lifetimes when women survive at least 30 years and men at least 20 years. One can see that, roughly, after values $x = 29$ and $y = 39$, the ratios $\Psi_1(x, y)$ remain constant. This happens since for very large survival times x, y , marginal survival



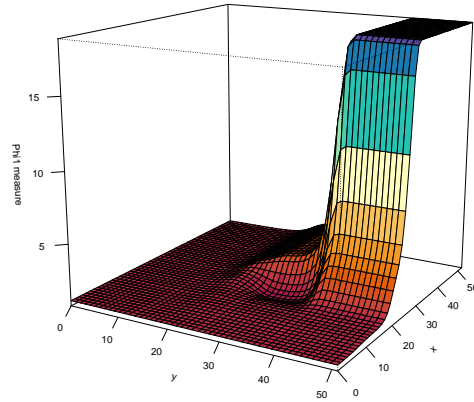
(A) Couple 1



(B) Couple 2



(C) Couple 3



(D) Couple 4

FIGURE 4.6. $\Psi_1(x, y)$ for the four couples.

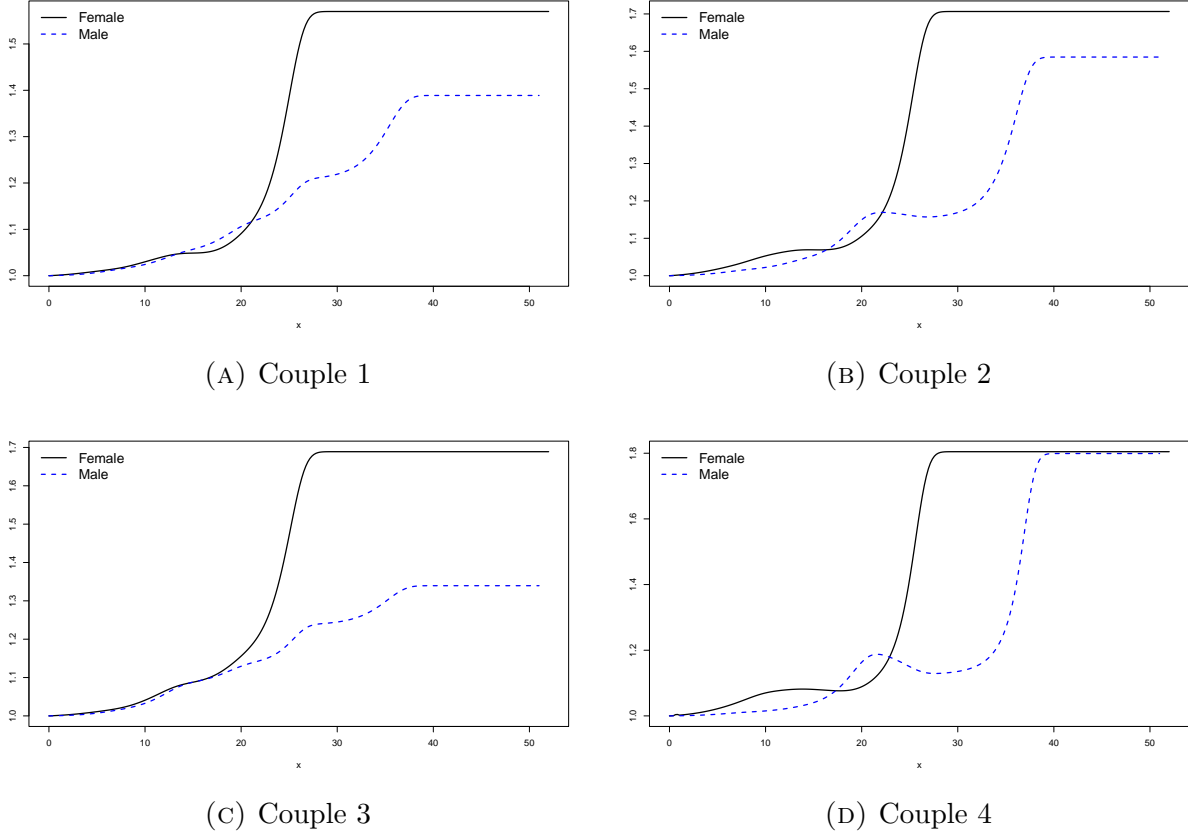
probabilities change very little, and this change is absorbed by $S(x, y)$.

Next, we depict in Figure 4.7 the measures

$$\Psi_2^1(0, x) = \mathbb{E}(Y_1 \mid Y_2 \geq x) / \mathbb{E}(Y_1),$$

$$\Psi_2^2(x, 0) = \mathbb{E}(Y_2 \mid Y_1 \geq x) / \mathbb{E}(Y_2)$$

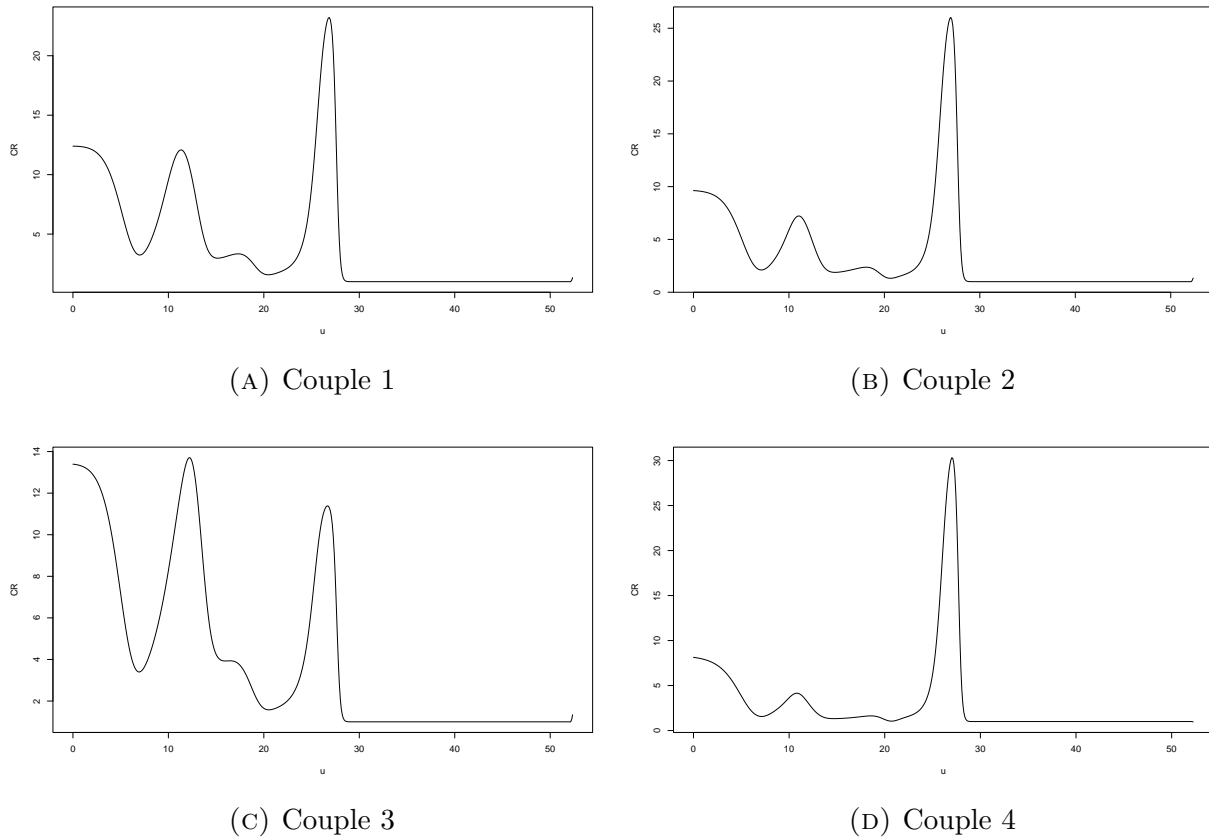
for all four couples, which give the relative change of conditional expectations of spouses' excess lifetimes, given that the partner survives at least x years. We see that the latter increase throughout with x . In general, the ratios $\Psi_2^i(\cdot, \cdot)$, $i = 1, 2$, are close in value when $x \leq 20$, meaning that the survival of a spouse has a similar effect on the remaining lifetime of the partner for the first 20 years. After that, the relative lifetime improvement increases much faster for women, i.e. their expected lifetime improvement is then more sensitive to the survival of the partner than vice versa. Like in Figure 4.6, both ratios remain constant after spouses' survival times of $x = 29$ for women and $x = 39$ for men.

FIGURE 4.7. $\Psi_2^1(0, y)$ and $\Psi_2^2(x, 0)$ for the four couples.

The last measure of time-dependent association we consider here is the cross-ratio

$$CR(x, y) = S(x, y) \frac{\frac{d^2}{dx dy} S(x, y)}{\frac{d}{dx} S_{Y_1}(x) \frac{d}{dy} S_{Y_2}(y)}$$

originally introduced by Clayton [9], which gives the relative increase of the force of mortality of an individual immediately after death of the partner. The quantity relevant in our model is $CR(u, u)$, and Figure 4.8 depicts the resulting figures for our model. In Luciano et al. [16], the resulting curves were monotone increasing in u , as a result of the imposed copula assumption on the joint lifetimes. In contrast, in the present setup these curves are not monotone increasing in u . One may interpret that in the present approach the a priori dependence assumptions are less specified, and the data have a stronger impact on the resulting shape of $CR(u, u)$ than in a specified copula model, where the data merely influence the value of the dependence parameter. One can see from Figure 4.8 that the cross-ratios exceed 1 for $u \leq 29$, so the survivor's force of mortality is increased immediately after the death of the spouse, showing a bereavement effect (or broken-heart syndrome), but not a monotone one (with the magnitude varying across age combinations of the couple). This bereavement effect somewhat seems to disappear for survival times beyond 29 years, but in that range survival probabilities are very low anyway, and there are very few data points in that range to draw strong conclusions.

FIGURE 4.8. $CR(u, u)$ for the four couples.

Eventually, like in many other situations, it may depend on the number of available data points whether one prefers to have a flexible dependence structure in the fitting or a pre-specified copula family with possibly attractive stylized features, especially for extrapolated conclusions in regions with few data points. In this discussion, one may still appreciate the immediate causal interpretation of the mIPH model in terms of a common ageing mechanism.

4.5. Life expectancies. Let us finally also use the model fit to get some insight into expected remaining lifetimes in the couple. Using Property (2.4), we are able to derive expected survival times for an individual, conditional on the survival time of their partner. Moreover, using optimal regression coefficients found by Algorithm 1 (Table 4.1) we can study how marginal expectations vary with ages in a couple. Letting the man's and woman's age vary from age 60 to 100, we get for each age combination a distinct mIPH distribution for the random vector \mathbf{Y} . Given these distributions, we summarise in Figure 4.9 how the expected remaining lifetime at issuance changes as a function of the male's and female's age at that point in time. For both man and woman, the marginal expected survival times decrease when both individuals in the couple grow older. For any specific age, both men and women have larger marginal expectations as their spouses become younger. That marginal expectation varies more for women, as one can see from the steepness and range

of the women's curve in Figure 4.9. Another way to interpret this is that men's expected survival times are affected less by the age of their partner, compared to women.

Besides age, conditioning also on the survival time of the spouse affects the initial

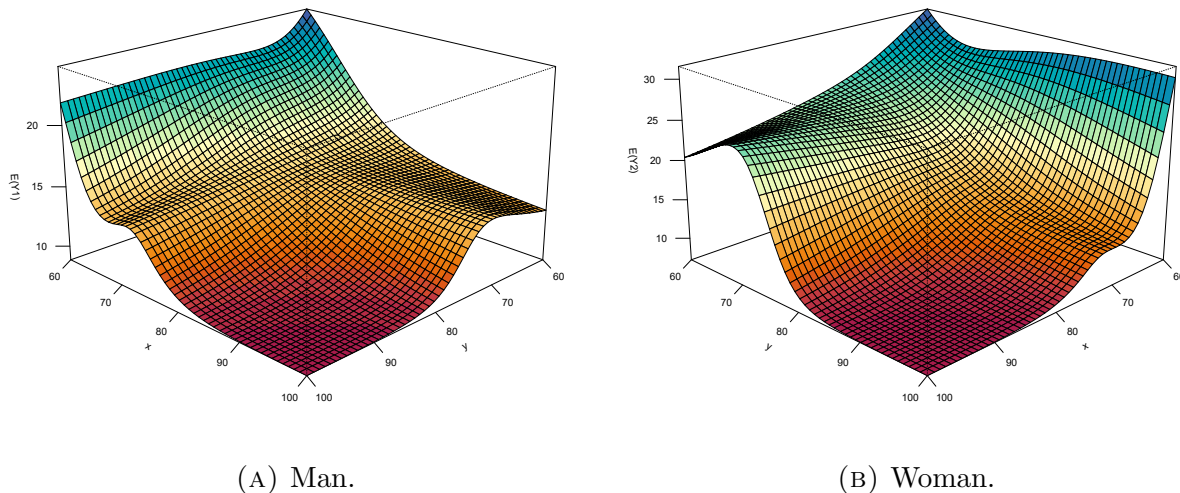


FIGURE 4.9. Marginal expected excess survival times as a function of the man's age (x) and woman's age (y) at issuance.

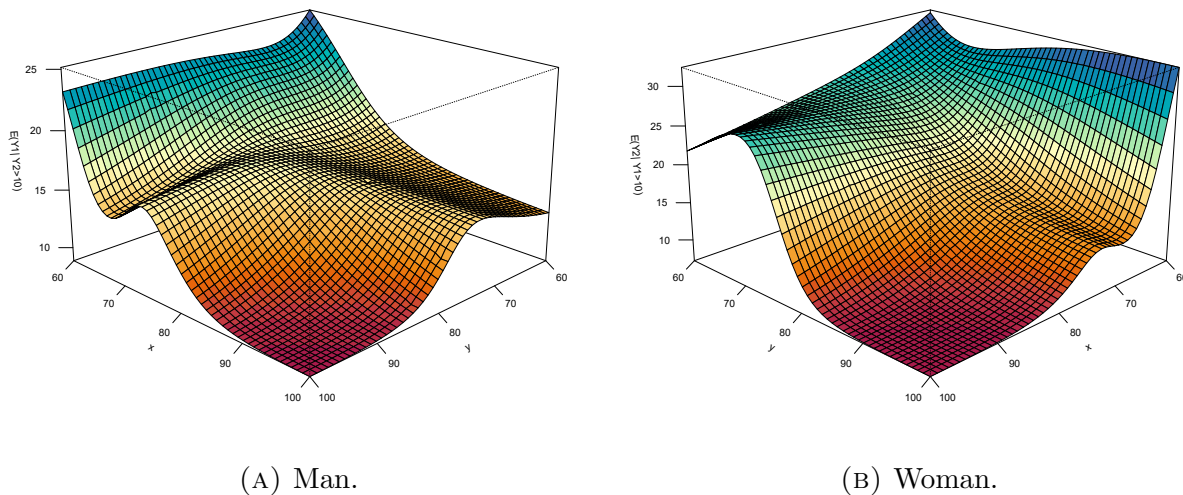


FIGURE 4.10. Marginal expected excess survival times, given that the spouse survives for at least 10 years.

distribution vector, leading to different expected values. Figures 4.10 and 4.11 present marginal expected survival times, conditional on a spouse survival of at least 10 and 15 years counted from issuance of the policy, respectively. The respective change in the men's remaining life expectation is notable by mere visual comparison, whereas for women it is less pronounced. From Figure 4.10 we see that the expectation increases for almost all

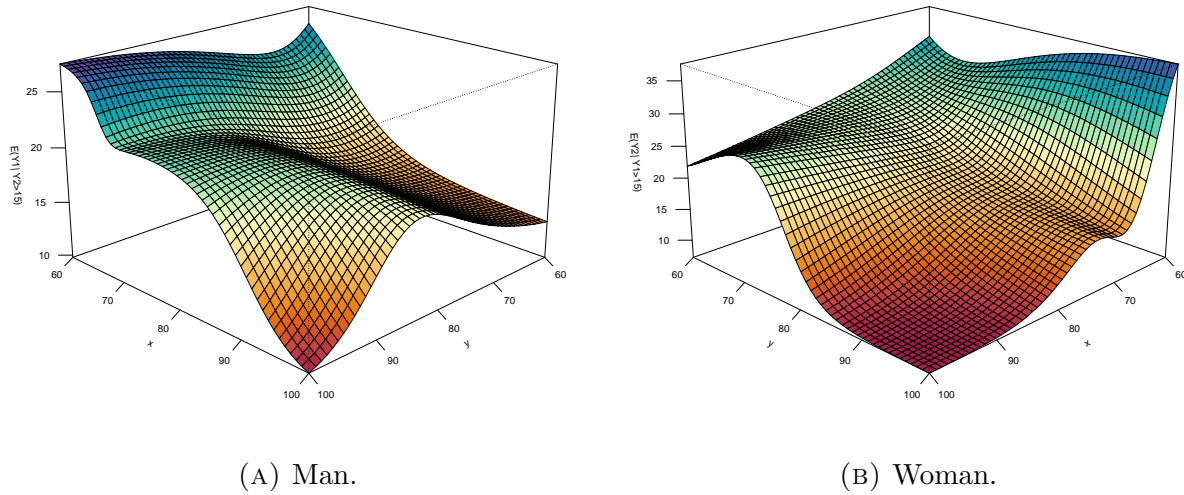


FIGURE 4.11. Marginal expected excess survival times, given that the spouse survives for at least 15 years.

ages. For men, one notices that the shape of the curve is changed for ages $65 \leq x \leq 75$. Moreover, for older ages x and y the curve is now steeper than before. In the women's case, marginal expectations for a woman aged 60 or 100 with husband aged 60 are now equivalent, and no other major change can be easily observed. The marginal expectation for men whose spouses survive at least 15 years are very much different from their unconditional counterparts. Inspecting Figure 4.11, one can see a sizeable change of the curve. Men with spouses of age $y \in (80, 100)$ are now expected to survive much longer than before, while once again for women we only have a rather minor twist of the curve. This may suggest that men's survival is more sensitive to their spouses' survival times than vice versa.

5. CONCLUSION

In this paper, we introduce the mIPH class, study some of its properties and develop an estimation procedure that allows for right-censored observations and covariate information. In particular, we use this framework to propose a bivariate Matrix-Gompertz distribution for the modelling of excess joint lifetimes of couples. Adapting a respective Expectation-Maximisation algorithm, we estimate sub-intensity matrices, inhomogeneity functions and different initial distribution vectors without separating joint features from marginals. Initial probabilities are assumed to be linked to spouses' ages at the issuance of an insurance policy. Employing multinomial logistic regressions to predict the latter, tailor-made bivariate distributions are produced that reflect distinct ageing dynamics and dependence structures. The resulting mIPH distributions showcase strong positive concordance for excess lifetimes of spouses, particularly when the difference in age at the issuance of the policy is small.

The results and illustrations given in this paper demonstrate the accuracy and flexibility of the mIPH class, which may also be employed in areas beyond the present lifetime setup, including applications in non-life insurance. The mIPH class may be considered preferable

to copula-based methods, particularly when one wants to estimate marginal and multivariate properties at the same time, and has sufficiently many data points available to keep the pre-imposed dependence assumptions (and structure) minimal. In addition, modelling with members of the mIPH class allows for an immediate causal interpretation of the resulting model in terms of common ageing through stages.

Acknowledgement. We would like to thank the Society of Actuaries, through the courtesy of Edward W. Frees and Emiliano Valdez for access to the data set used in this paper. Financial support from the Swiss National Science Foundation Project 200021_191984 is gratefully acknowledged.

REFERENCES

- [1] H. Albrecher and M. Bladt. Inhomogeneous phase-type distributions and heavy tails. *Journal of Applied Probability*, 56(4):1044–1064, 2019.
- [2] H. Albrecher, M. Bladt, M. Bladt, and J. Yslas. Mortality modeling and regression with matrix distributions. *arXiv preprint arXiv:2011.03219*, 2021.
- [3] H. Albrecher, M. Bladt, and J. Yslas. Fitting inhomogeneous phase-type distributions to data: the univariate and the multivariate case. *Scandinavian Journal of Statistics*, 49(1):44–77, 2022.
- [4] S. Asmussen, P. J. Laub, and H. Yang. Phase-type models in life insurance: Fitting and valuation of equity-linked benefits. *Risks*, 7(1), 2019.
- [5] S. Asmussen, O. Nerman, and M. Olsson. Fitting phase-type distributions via the em algorithm. *Scandinavian Journal of Statistics*, 23(4):419–441, 1996.
- [6] M. Bladt. A tractable class of multivariate phase-type distributions for loss modeling. *Preprint, University of Lausanne, arXiv preprint arXiv:2110.05179*, 2021.
- [7] M. Bladt and B. F. Nielsen. *Matrix-Exponential Distributions in Applied Probability*, volume 81. Springer, 2017.
- [8] M. Bladt and J. Yslas. Phase-type mixture-of-experts regression for loss severities. *Preprint, University of Lausanne, arXiv preprint arXiv:2110.05179*, 2022.
- [9] David G Clayton. A model for association in bivariate life tables and its application in epidemiological studies of familial tendency in chronic disease incidence. *Biometrika*, 65(1):141–151, 1978.
- [10] D. M. Dabrowska. Uniform consistency of the kernel conditional kaplan-meier estimate. *The Annals of Statistics*, 17(3):1157–1167, 1989.
- [11] F. Dufresne, E. Hashorva, G. Ratovomirija, and Y. Toukourou. On age difference in joint lifetime modelling with life insurance annuity applications. *Annals of Actuarial Science*, 12(2):350–371, 2018.
- [12] E. W. Frees, J. Carriere, and E. Valdez. Annuity valuation with dependent mortality. *The Journal of Risk and Insurance*, 63(2):229–261, 1996.
- [13] F. Gobbi, N. Kolev, and S. Mulinacci. Joint life insurance pricing using extended marshall-olkin models. *ASTIN Bulletin*, 49(2):409–432, 2019.
- [14] M. Ji, M. Hardy, and J. S.-H. Li. Markovian approaches to joint-life mortality. *North American Actuarial Journal*, 15(3):357–376, 2011.
- [15] X. S. Lin and X. Liu. Markov aging process and phase-type law of mortality. *North American Actuarial Journal*, 11(4):92–109, 2007.
- [16] E. Luciano, J. Spreeuw, and E. Vigna. Modelling stochastic mortality for dependent lives. *Insurance: Mathematics and Economics*, 43(2):234–244, 2008.
- [17] K. Moutanabbir and H. Abdelrahman. Bivariate Sarmanov phase-type distributions for joint lifetimes modeling. *Methodology and Computing in Applied Probability*, 24(2):1093–1118, 2022.
- [18] M. Olsson. Estimation of phase-type distributions from censored data. *Scandinavian Journal of Statistics*, 23(4):443–460, 1996.
- [19] J. Spreeuw and I. Owadally. Investigating the broken-heart effect: a model for short-term dependence between the remaining lifetimes of joint lives. *Annals of Actuarial Science*, 7(2):236–257, 2013.

DEPARTMENT OF ACTUARIAL SCIENCE, FACULTY OF BUSINESS AND ECONOMICS, UNIVERSITY OF LAUSANNE, UNIL-DORIGNY, 1015 LAUSANNE AND SWISS FINANCE INSTITUTE, 1015 LAUSANNE

Email address: `hansjoerg.albrecher@unil.ch`

DEPARTMENT OF ACTUARIAL SCIENCE, FACULTY OF BUSINESS AND ECONOMICS, UNIVERSITY OF LAUSANNE, UNIL-DORIGNY, 1015 LAUSANNE

Email address: `martin.bladt@unil.ch`

DEPARTMENT OF ACTUARIAL SCIENCE, FACULTY OF BUSINESS AND ECONOMICS, UNIVERSITY OF LAUSANNE, UNIL-DORIGNY, 1015 LAUSANNE

Email address: `alaric.mueller@unil.ch`